Journal of Membrane Science, 26 (1986) 165–178
Elsevier Science Publishers B.V., Amsterdam — Printed in The Netherlands

RESISTANCE TO THE PERMEATE FLUX IN UNSTIRRED ULTRAFILTRATION OF DISSOLVED MACROMOLECULAR SOLUTIONS

S. NAKAO*, J.G. WIJMANS and C.A. SMOLDERS

Department of Chemical Technology, Twente University of Technology, P.O. Box 217, 7500 AE Enschede (The Netherlands)

(Received April 30, 1985; accepted in revised form August 28, 1985)

Summary

The flux decline during the unstirred ultrafiltration of dissolved macromolecular solutions such as polyethylene glycol and dextran solutions was measured at different pressures from 1 to 4 × 10^5 Pa and different bulk concentrations from 0.1 to 0.55 kg/m^3 with three types of polysulfone membranes. On the basis of the concept that a concentrated solution layer (not a gel layer) is formed on the membrane surface, the hydraulic resistance of the boundary layer was defined with the help of solvent permeability of dissolved macromolecules. The cake filtration theory was employed to analyze the flux decline behaviour. This simple theory worked well and the effective boundary layer concentrations calculated with the boundary layer resistance model developed here were physically quite reasonable. The calculated boundary layer concentrations depend on the applied pressure. The origin of this dependency might be the step concentration profile assumed in the cake filtration theory.

Introduction

Ultrafiltration is one of the best techniques for the concentration of macromolecular solutions. Attempts — largely unsuccessful — have also been made to employ ultrafiltration to fractionate such solutions. One major problem in practical applications is the permeate flux which declines during operation. In a membrane separation process, solute molecules conveyed toward the membrane are rejected by the membrane and accumulate very near to the membrane surface, and a part of them diffuses back to the bulk along the concentration profile. This phenomenon is well-known as concentration polarization.

In case of ultrafiltration of macromolecular solutions, the amount of solute diffusing back is usually very small because of the small diffusion coefficients, and as a result the concentration at the membrane surface becomes very high. This increased concentration causes an enormous flux decline, and it has been tried to describe this with two quite different models. One

*Present address: Institute of Industrial Science, University of Tokyo, 7-22-1 Roppongi, Minato-ku, Tokyo, Japan.

0376-7388/86/$03.50

is the gel layer model [1—7] in which the extra hydraulic resistance of a gel layer in addition to the membrane resistance reduces the flux, and the other is the osmotic pressure model [8—15] in which the applied pressure is reduced by the osmotic pressure and the decreased driving force causes the flux decline.

The physical definition of a gel layer has not been clear even in the analysis based on the gel layer model. It could be expected that the true gel has a sharp phase boundary, zero diffusion coefficient and well-defined melting point [15], and that it has no fluidity. According to this definition, it might be supposed that a true gel layer is not formed in the ultrafiltration of macromolecular solutions except for some proteins which are known to give gels. Therefore, the layer built up on the membrane surface should be viewed upon as a concentrated macromolecular solution layer.

There are two ways to account for the influence of this boundary layer on the permeate flux. The first is to evaluate the solute concentration at the membrane surface and to calculate the decrease in the effective driving force due to the osmotic pressure. This is the osmotic pressure model approach. Recently, we have shown that the osmotic pressure model strongly resembles the gel layer model in situations where concentration polarization is severe [16].

The second way is to calculate the resistance of the boundary layer, which is possible if the concentration profile and the solvent permeability of the dissolved macromolecules are known [17, 18]. In this hydraulic resistance model, the total resistance for the permeate flow is the sum of this boundary layer resistance and the membrane resistance.

On theoretical grounds, it can be shown that the two approaches mentioned above are equivalent [15, 18, 19].

In the present work, the boundary layer resistance model was used to analyze the flux decline during the unstirred ultrafiltration of dissolved macromolecular solutions. Assuming a step concentration profile and a time-independent concentration in the boundary layer (only the layer thickness increases with time), the cake filtration theory was employed to calculate the change of the resistance with time. The permeability was measured with an ultracentrifuge method [17].

Theory

In case of steady state flow or stirred ultrafiltration, the amount of solute which diffuses away from a membrane surface is balanced by the amount conveyed toward a membrane by the permeate flow. Thus, the steady state flux is written with the following so-called concentration polarization equation [1, 2, 4]

$$J_v = k \ln \frac{C_m - C_p}{C_b - C_p} \tag{1}$$

The mass transfer coefficient k is determined by the flow or stirring condition and the characteristics of solute and solution. The basis of this derivation is the diffusion phenomenon.

It is also possible to explain the flux decline on the basis of the resistance phenomenon, and the permeate flux is then written using the hydraulic resistance of the boundary layer R_{bl}

$$J_v = \frac{1}{A}\frac{dV}{dt} = \frac{1}{\mu}\frac{\Delta P}{R_m + R_{bl}} \tag{2}$$

Equations (1) and (2) must give the same flux under the same conditions. Thus, one can expect that there must be a certain relationship between C_m and R_{bl}. Nakao et al. [3] reported this relationship for polyvinylalcohol and ovalbumin. They used the term gel layer resistance, but they did not clarify the physical meaning of R_{bl}. Furthermore, flow or stirred system experiments make the analysis more complicated because the influence of mass transfer phenomena must be analyzed. Therefore, for the analysis of concentration polarization and flux decline in ultrafiltration of macromolecular solutions, it is very important to know the physical meaning of R_{bl}, and an unstirred system is suitable for this purpose.

Assuming a step concentration profile and a time-independent concentration C_{bl} in the boundary layer, the boundary layer resistance is written as

$$R_{bl} = \delta\, r_{bl} \tag{3}$$

where δ is the boundary layer thickness increasing with time. The rejection of dissolved macromolecules, especially when using dissolved linear chain macromolecules is not always 100%. Thus, according to the cake filtration theory, the solute mass balance is written as

$$C_b R_{obs} V = \delta A\, C_{bl} \tag{4}$$

where R_{obs} is the observed rejection ($R_{obs} = 1 - C_p/C_b$). Substitution of eqns. (3) and (4) into eqn. (2) gives

$$\frac{dt}{dV} = \frac{\mu R_m}{A\Delta P} + \frac{\mu\, C_b\, R_{obs}}{A^2\, \Delta P}\,\frac{r_{bl}}{C_{bl}}\,V \tag{5}$$

or

$$\frac{1}{j_v} = \frac{1}{J_w} + \frac{\mu\, C_b\, R_{obs}}{\Delta P}\,\frac{r_{bl}}{C_{bl}}\,v \tag{6}$$

where j_v is an unsteady state permeate flux and v is a specific cumulative filtration volume ($v = V/A$).

Mijnlieff and Jaspers [17] developed the relationship between solvent permeability of dissolved polymeric material and its sedimentation coefficient. This permeability could be applied, for instance, to the solvent permeation

through a concentrated polymer solution in a cell, in which the solution is kept in position by two membranes which are permeable to the solvent and impermeable to macromolecules. The boundary layer studied here is almost identical to such a solution, so we used the concept of solvent permeability to calculate the specific resistance of the boundary layer.

Mijnlieff and Jaspers [17] derived

$$r_{bl} = \frac{1}{p_{bl}} = \frac{1 - \bar{v}\rho_w}{\mu_w} \frac{C_{bl}}{s} \tag{7}$$

The sedimentation coefficient is a function of concentration. Now the unknown quotient r_{bl}/C_{bl} in eqn. (5) or eqn. (6) can be written with only one variable C_{bl}

$$\frac{r_{bl}}{C_{bl}} = \frac{1 - \bar{v}\rho_w}{\mu_w} \frac{1}{s(C_{bl})} \tag{8}$$

In this study, the sedimentation coefficient was measured as a function of concentration by the ultracentrifuge method, and the boundary layer concentration was calculated from the slope of $1/j_v$ vs. v plot using eqns. (6) and (8).

Experiments

Unstirred ultrafiltration experiments

The unstirred experiments were carried out with the apparatus shown in Fig. 1. The membrane holder used is a Millipore filter holder (effective membrane area is $1.38 \times 10^{-3}\,m^2$). Before the membrane is sealed, the feed solution is slightly pressurized and the air present in the holder flows away. The feed solution does not permeate through the membrane during this procedure. Then the membrane is sealed and the feed solution is pressurized to a certain pressure as soon as possible. The zero time of the measurement is defined as the time when pressurization starts. Volume filtrated is measured with time.

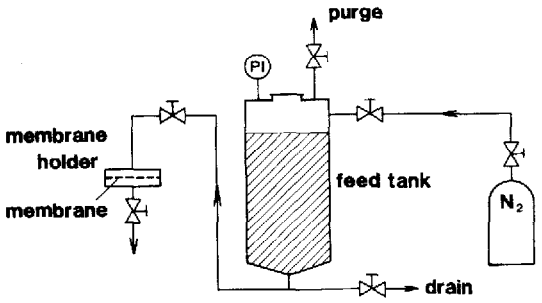

Fig. 1. Experimental apparatus, schematically.

Three types of polysulfone membranes were used. Two of them are commercially available ultrafiltration membranes (WFS 600 and WFS 900) manufactured by Wafilin B.V., The Netherlands. Another one was made in our laboratory by the immersion precipitation method from a casting solution of polysulfone, methyl cellosolve and DMAc (18:7:75 in weight %). The coagulant was water. Macromolecular solutes used are Dextran T500 (M_w = 465,000, Pharmacia Fine Chemicals) and polyethylene glycol PEG 600 (M_w = 600,000, Polysciences, Inc.).

The pure water flux of these membranes, measured with ultrafiltered water, decreased very much after the performance of ultrafiltration experiments with macromolecular solutions and it did not return to the initial value after washing the membrane surface. It was supposed that this flux decline was caused by the plugging of membrane pores. The decreased flux became constant after a certain number of experiments, and then the flux decline with time was measured at several different applied pressures, 1 to 4 × 10^5 Pa. The concentration range of the feed solution was from 0.1 to 0.55 kg/m^3. The solute concentration was measured by a Beckman model 915A Total Organic Carbon Analyzer. The temperature during the experiments was 20° C.

Measurements of the sedimentation coefficient

Sedimentation experiments were carried out using a Beckman model E analytical ultracentrifuge, equipped with a Schlieren optics and temperature control system. Centerpieces of 1.5, 3 and 12 mm were used, and the rotation speed and measurement temperature were 48,000 min^{-1} and 20° C, respectively. The sedimentation coefficients were determined from the displacement of the maximum of the concentration gradient curve. The concentration range was from 4.6 to 150 kg/m^3.

In order to calculate the specific resistance from the sedimentation coefficient using eqn. (7), the partial specific volume $\bar{v}$ was also determined. The solution density was measured at several concentrations using a Digital Precision Density Meter model DMA 50 (Anton Paar K.G., Austria) at 20° C, and then $\bar{v}$ was calculated from the slope of the density vs. concentration plot.

Results and discussion

Rejection

The observed rejection changed with cumulative filtration volume at the beginning of the measurement as is shown in Fig. 2, and then it became almost constant under all experimental conditions. It is very difficult to find the cause of this rejection change, because it was almost impossible to measure the permeate concentration exactly at the beginning of the experiments. Before the experiment was started, the air present in the cell was purged with feed solution, and then the membrane was sealed. Thus, a part of the

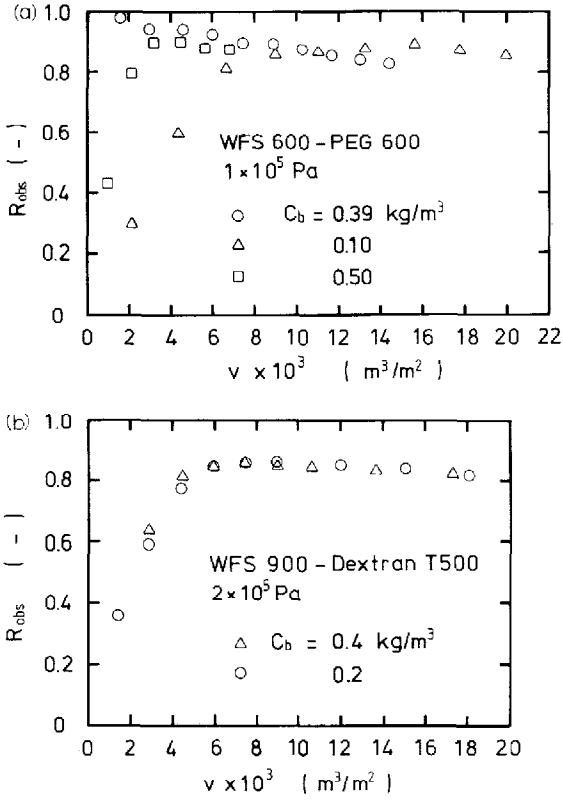

Fig. 2. Changes of the observed rejection with the specific cumulative volume: (a) PEG 600 solutions — in the experiment indicated with circles, the permeate side of the cell was washed with pure water after the membrane was sealed; (b) Dextran T500 solutions — permeate side has not been washed with pure water.

feed solution might have flowed into the permeate side of the cell during this procedure, making the initial rejection low. It has also been tried to wash the permeate side with pure water after the membrane was sealed. In this case, pure water remaining in the permeate side influenced the rejection and a high rejection resulted. Finally, it was assumed for the analysis that the rejection might be constant from the beginning of the experiment. The rejection of WFS 600 membrane was 85% to PEG 600 and 45% to Dextran T500, while the rejection of WFS 900 membrane was 83% to Dextran T500. A laboratory made membrane rejected 70% of Dextran T500. These rejections were almost the same in all experiments.

Flux decline during ultrafiltration

Results of ultrafiltration of PEG 600 and Dextran T500 solutions under various experimental conditions are illustrated in Figs. 3 and 4 by means of $1/j_v$ vs. v plots according to eqn. (6). Figure 3 shows the influence of feed

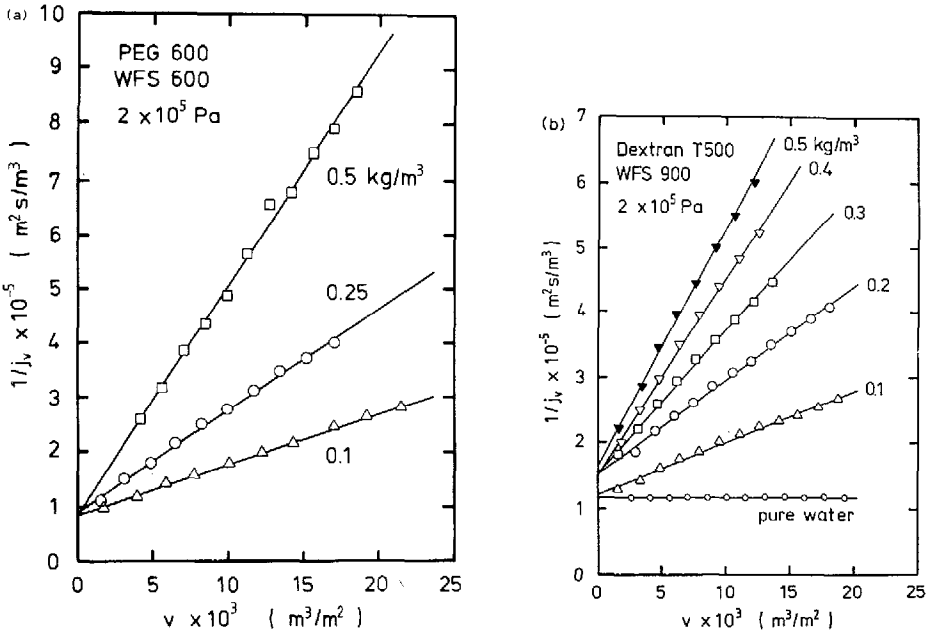

Fig. 3. Reciprocal flux as a function of the specific cumulative volume and the influence of the bulk concentration: (a) PEG 600 solutions; (b) Dextran T500 solutions.

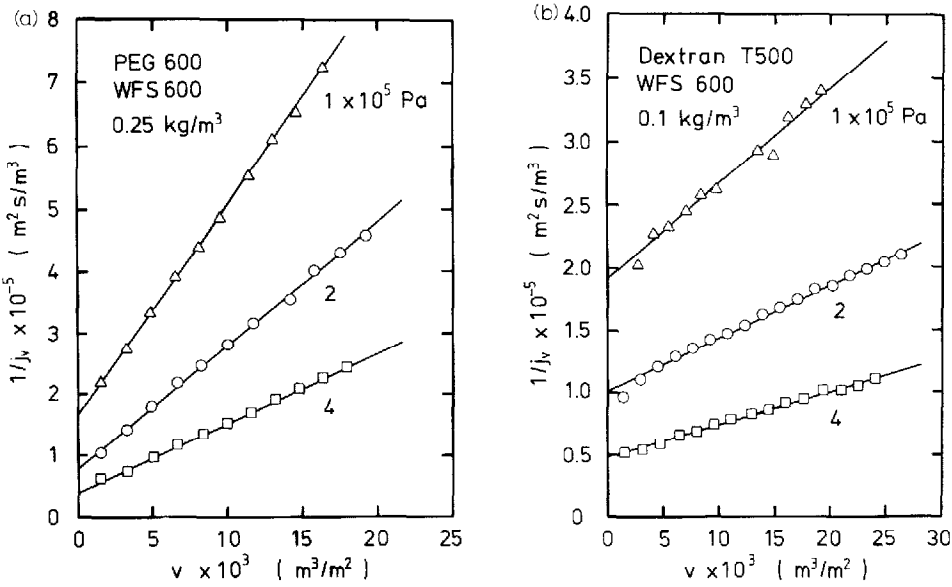

Fig. 4. Reciprocal flux as a function of the specific cumulative volume and the influence of the applied pressure: (a) PEG 600 solution; (b) Dextran T500 solution.

concentration, while Fig. 4 shows the influence of applied pressure. It is remarkable that for both solutions a straight line can be drawn for any bulk concentration and pressure and for all membranes. Intercepts of these lines were independent of the bulk concentration and almost the same under the same pressure as shown in Fig. 3. The intercept was almost in proportion to the reciprocal value of the applied pressure as shown in Fig. 4. The agreement between these intercepts and reciprocals of pure water flux was also very good, and this is expected by eqn. (6).

The slopes of the lines in Figs. 3 and 4 indicate the rate of flux decline and are affected by the bulk concentration, applied pressure, temperature which affects the viscosity, solute rejection and boundary layer concentration. As illustrated in Figs. 3 and 4 a higher bulk concentration, a lower applied pressure and a higher solute rejection give a larger slope. However, with the help of r_{bl}/C_{bl} values, it is possible to analyze the flux decline rate quantitatively without influences of experimental conditions.

Flux decline index

The flux decline index r_{bl}/C_{bl} was calculated for all experiments from the slope of the $1/j_v$ vs. v plot, and it is shown in Fig. 5(a) for PEG 600 and in Fig. 5(b) for Dextran T500. It is quite obvious in both cases that r_{bl}/C_{bl} is almost constant with respect to the bulk concentration independent of the rejection. According to eqn. (6), this result means that the actual flux decline rate increases proportionally with the bulk concentration and solute rejection under the same pressure. It is also clear that there is an influence of applied pressure on the r_{bl}/C_{bl} value, and that the higher pressure gives the larger value. The effect of pressure in Dextran T500 solutions was larger than that in PEG 600 solutions.

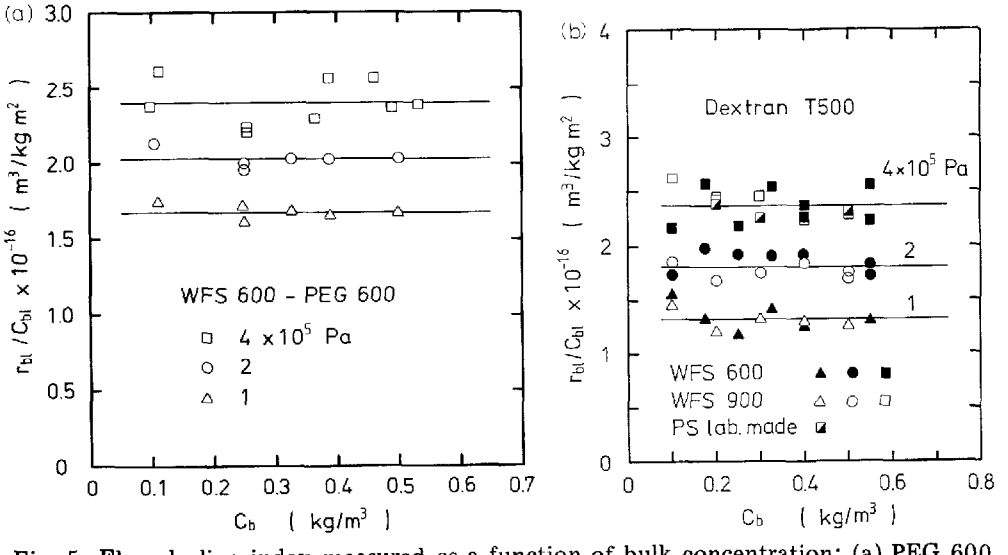

Fig. 5. Flux decline index measured as a function of bulk concentration: (a) PEG 600 solutions; (b) Dextran T500 solutions.

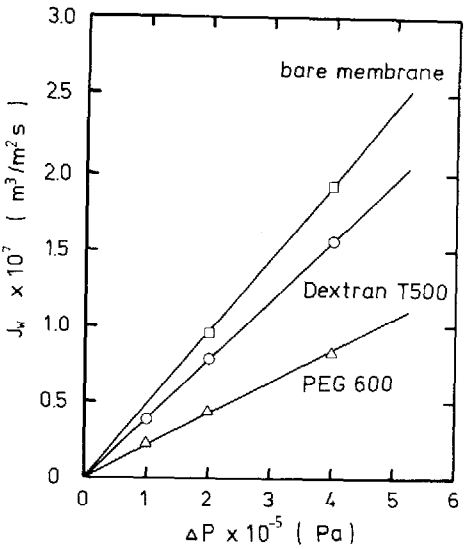

Fig. 6. Pure water fluxes measured with the bare membrane and with the membrane having a boundary layer of PEG 600 and Dextran T500 solutions.

One possible reason of this pressure dependency is the compressibility of a concentrated boundary layer. In order to measure this compressibility, the feed solution was immediately changed to pure water after an ultrafiltration experiment at 1×10^5 Pa. Then, the pure water flux was measured at three different pressures (1, 2 and 4×10^5 Pa) with the membrane on which the concentrated boundary layer still remained. If the boundary layer was compressible, the pure water flux should vary less than proportionally with the applied pressure. The pure water flux measured at 1×10^5 Pa for the membrane including the boundary layer must be equal to the final flux in the ultrafiltration experiment. In both cases (Dextran T500 and PEG 600) the pure water flux was larger than the ultrafiltration flux. The reason for this difference might be that a part of the boundary layer was washed away from the membrane surface during the change of the feed solution. Anyhow, it is quite obvious from Fig. 6 that the flux is lower than that measured with the bare membrane because of the extra resistance of the boundary layer, and that it is proportional to the applied pressure. It can be concluded that both PEG 600 and Dextran T500 boundary layers do not have any compressibility, and the influence of pressure will be discussed below.

Sedimentation coefficient and resistance of a boundary layer

In order to investigate the validity of the hydraulic resistance model, it is very interesting and important to know the boundary layer concentration. As explained in the analysis section, this calculation can be carried out using sedimentation coefficient data.

Sedimentation coefficients for Dextran T500 solutions measured at 20° C

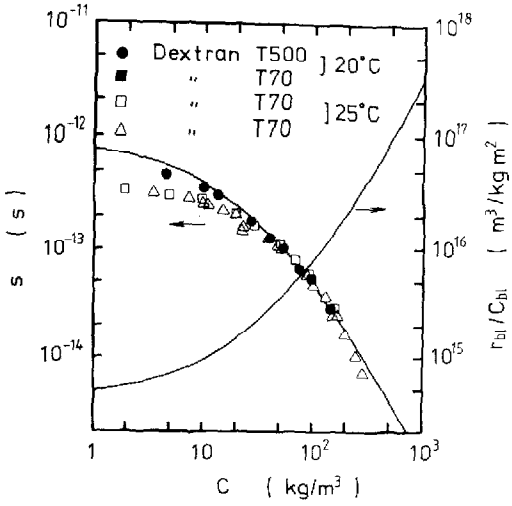

Fig. 7. The sedimentation coefficients and the value of r_{bl}/C_{bl} as a function of concentration; curves have been drawn according to eqn. (11) for s and eqn. (12) for r_{bl}/C_{bl}. □, △: Data taken from Refs. [18, 20].

are plotted in Fig. 7 together with literature data for Dextran T70 (M_w about 70,000) which were measured at 25°C [18, 20]. In order to estimate the influence of temperature, the sedimentation coefficient, s, of Dextran T70 solutions was also measured at 20°C with the same method used for Dextran T500 and plotted in Fig. 7. It is quite clear that the difference in s due to a temperature difference of 5°C can be neglected within experimental error.

The sedimentation coefficient depends on the molecular weight of the solute in the dilute region, but above the overlap concentration for the macromolecule the sedimentation coefficient becomes independent of the molecualr weight [21]. Results illustrated in Fig. 7 show this molecular weight independency above the overlap concentration of Dextran T70 which is about 40 kg/m³, and this also means that the measurements were accurate enough.

In the low concentration region, the concentration dependency of sedimentation coefficients is generally expressed with the following equation.

$$1/s = (1/s_0)(1 + k_s C) \tag{9}$$

At higher concentration eqn. (9) is not adequate to represent the concentration dependency, and a second order term is usually added

$$1/s = (1/s_0)(1 + k_s C + k_s' C^2) \tag{10}$$

Sedimentation coefficients were not measured at low concentration in this work, thus s_0 and k_s for Dextran T500 solutions were determined by the interpolation of literature data where different molecular weight Dextrans had been measured [22—24]. Then, k_s' was determined by curve fitting of eqn. (10) to the available data. Literature data of Dextran T70 above the

overlap concentration were also used for this fitting. The concentration dependency obtained is expressed as

$$1/s = (1 + 106\,C + 617\,C^2)/(8.5 \times 10^{-13}) \quad (11)$$

and a solid line in Fig. 7 is drawn with this equation.

The measured partial specific volume of Dextran T500 is 6.25×10^{-4} m^3/kg and this value agrees well with literature data of Dextran T70 [18, 20]. The specific resistance of Dextran T500 solutions can now be calculated and eqn. (8) becomes

$$r_{bl}/C_{bl} = 4.40 \times 10^{13}\ (1 + 106\,C + 617\,C^2) \quad (12)$$

where literature values for pure water density and viscosity are used. This equaton is also represented in Fig. 7. The flux decline index r_{bl}/C_{bl} increases rapidly above the overlap concentration which is about 20 kg/m^3 for Dextran T500.

Boundary layer concentration

Effective boundary layer concentrations were calculated using eqn. (12) for all experiments of Dextran T500, and results are plotted in Fig. 8. Calculated values depended on the applied pressure and varied from 146 to 219 kg/m^3. This concentration range seems to be physically quite reasonable as the concentration of dissolved macromolecules in the boundary layer. The range of polyvinylalcohol (M_w = 100,000) boundary layer concentrations has been reported to be from 10 to 100 kg/m^3 [3], and the calculated concentrations based on the osmotic pressure model were 50 to 100 kg/m^3 for polyethylene glycol (M_w = 15,500) [9] and 150 to 450 kg/m^3 for various molecular weight Dextrans (M_w = 21,800–100,500) [9]. These data were obtained in flow or stirred ultrafiltration experiments. Solutions with concentrations equivalent to the boundary layer concentrations shown above are fluid. This indicates that no gel layer has been formed

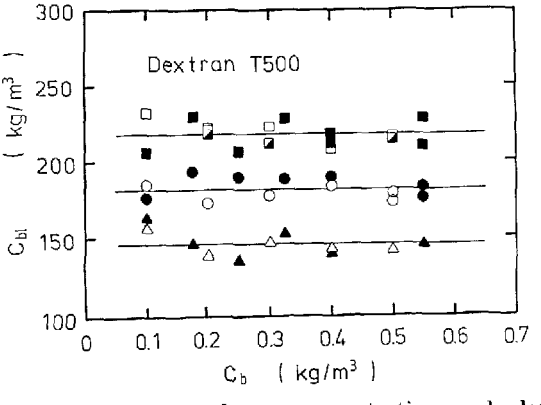

Fig. 8. Boundary layer concentrations calculated with the boundary layer resistance model (keys are the same as in Fig. 5(b)).

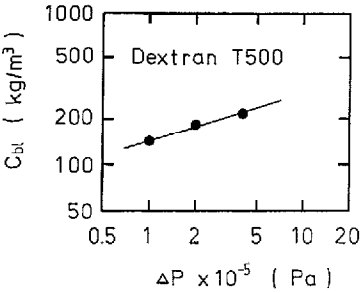

Fig. 9. Effect of the applied pressure on the boundary layer concentration.

in these systems. This is also the reason why the boundary layer is not compressible, because fluids normally do not have compressibility under these circumstances.

The influence of applied pressure on the boundary layer concentration is illustrated in Fig. 9. It is very difficult to quantify this pressure effect only from our experimental results. In this study, a step concentration profile was assumed and the effect of back diffusion was not considered. However, the concentration profile near the membrane surface is the result of a balance between the amount of macromolecules conveyed toward the membrane by the permeate flux and the amount diffusing back to the bulk. The former amount depends on the applied pressure, while the latter amount depends on both the diffusion coefficient and the concentration profile. Therefore, an analysis in which the concentration profile is not reduced to a step function but in which the true profile is employed, may explain the observed pressure effect. This approach will be undertaken and the results will be published in a forthcoming paper.

Conclusions

In order to clarify the physical meaning of the extra resistance to the permeate flux during the ultrafiltration of dissolved macromolecular solutions, the flux decline was measured using an unstirred cell. Since the experimental results showed a flux decline comparable to the flux decline in the ultrafiltration of colloidal particle solutions, they were analyzed with the cake filtration theory which usually worked well for colloidal particle solutions.

In the analysis, it was assumed that no gel layer was formed but that a concentrated boundary layer was built up near the membrane surface. This boundary layer still possesses all properties of a fluid system. Therefore, the solvent permeability of dissolved macromolecules which was calculated from sedimentation measurements was applied to analyze the hydraulic resistance of the boundary layer. The effective boundary layer concentration calculated with this boundary layer resistance model varied from 146 to 219 kg/m^3 for Dextran T500, and these values seemed physically quite reasonable. Furthermore, the fact that solutions with concentrations upto 400 kg/m^3

are clearly fluid confirmed the validity of the assumption that a gel layer was not formed.

Boundary layer concentrations showed the influence of the applied pressure (higher concentrations at higher pressures), and it is supposed that this influence was caused by the step concentration profile assumed in the cake filtration theory.

List of symbols

A membrane area (m^2)
C concentration (kg/m^3)
J_v steady state flux (m^3/m^2-sec)
j_v unsteady state flux (m^3/m^2-sec)
k mass transfer coefficient (m/s)
k_s constant in eqns. (9) and (10) (m^3/kg)
k_s' constant in eqn. (10) (m^6/kg^2)
ΔP applied pressure (Pa)
p solvent permeability of dissolved macromolecule (m^2)
R hydraulic resistance (1/m)
R_{obs} observed rejection ($= 1 - C_p/C_b$)
r specific resistance ($1/m^2$)
s sedimentation coefficient (sec)
s_0 sedimentation coefficient at zero concentration (sec)
t time (sec)
V cumulative filtration volume (m^3)
v specific cumulative filtration volume (m^3/m^2)
$\bar{v}$ partial specific volume (m^3/kg)

Greek symbols
δ boundary layer thickness (m)
ρ density (kg/m^3)
μ viscosity (Pa-sec)

Subscripts
b bulk
bl boundary layer
m membrane
p permeate
w water

References

1 W.F. Blatt, A. Dravid, A.S. Michaels and L. Nelsen, Solute polarization and cake formation in membrane ultrafiltration: Causes, consequences and control techniques, in: J.E. Flinn (Ed.), Membrane Science and Technology, Plenum Press, New York, 1970, p. 47.

2 A.S. Michaels, New separation technique for the CPI, Chem. Eng. Progress, 64(12) (1968) 31.
3 S. Nakao, T. Nomura and S. Kimura, Characteristics of macromolecular gel layer formed on ultrafiltration tubular membrane, AIChE J., 25 (1979) 615.
4 M.C. Porter, Concentration polarization with membrane ultrafiltration, Ind. Eng. Chem. Product Res. Develop., 11 (1972) 234.
5 R.F. Probstein, J.S. Shen and W.F. Leung, Ultrafiltration of macromolecular solutions at high polarization in laminar flow, Desalination, 24 (1978) 1.
6 J.J.S. Shen and R.F. Probstein, On the prediction of limiting flux in laminar ultrafiltration of macromolecular solutions, Ind. Eng. Chem. Fundam., 16 (1977) 459.
7 D.R. Trettin and M.R. Doshi, Ultrafiltration in an unstirred batch cell, Ind. Eng. Chem. Fundam., 19 (1980) 189.
8 M.J. Clifton, N. Abidine, P. Aptel and V. Sancez, Concentration polarization in ultrafiltration: The development of a new model, lecture presented at the International Membrane Technology Conference, Sydney, Australia, 1983.
9 R.L. Goldsmith, Macromolecular ultrafiltration with microporous membranes, Ind. Eng. Chem. Fundam., 10 (1971) 113.
10 A.A. Kozinski and E.N. Lightfoot, Protein ultrafiltration: A general example of boundary layer filtration, AIChE J., 18 (1972) 1030.
11 W.F. Leung and R.F. Probstein, Low polarization in laminar ultrafiltration of macromolecular solutions, Ind. Eng. Chem. Fundam., 18 (1979) 274.
12 G. Mitra and J. Lundblad, Ultrafiltration of immune serum globulin and human serum albumin: Regression analysis studies, Sep. Sci. Technol., 13 (1978) 89.
13 D.R. Trettin and M.R. Doshi, Pressure-independent ultrafiltration — Is it gel limited or osmotic pressure limited?, ACS Symp. Ser., 154 (1981) 373.
14 V.L. Vilker, C.K. Colton and K.A. Smith, Concentration polarization in protein ultrafiltration, part II: Theoretical and experimental study of albumin ultrafiltered in an unstirred cell, AIChE J., 27 (1981) 637.
15 M. Wales, Pressure drop across polarization layers in ultrafiltration, ACS Symp. Ser., 154 (1981) 159.
16 J.G. Wijmans, S. Nakao and C.A. Smolders, Flux limitation in ultrafiltration: Osmotic pressure model and gel layer model, J. Membrane Sci., 20 (1984) 115.
17 P.F. Mijnlieff and W.J.M. Jaspers, Solvent permeability of dissolved polymer material. Its direct determination from sedimentation measurements, Trans. Faraday Soc., 67 (1971) 1837.
18 J.G. Wijmans, S. Nakao and C.A. Smolders, Hydrodynamic resistance of concentrated polarization boundary layers in ultrafiltration, J. Membrane Sci., 22 (1985) 117.
19 P. Dejmek, Concentration polarization in ultrafiltration of macromolecules, Ph.D. Thesis, Lund Institute of Technology, Lund, Sweden, 1975.
20 W. Brown, P. Stilbs and R.M. Johnsen, Self-diffusion and sedimentation of Dextran in concentrated solutions, J. Polym. Sci., Polym. Phys. Ed., 20 (1982) 1771.
21 J. Roots and B. Nystrom, Application of scaling concepts to sedimentation phenomena in semidilute macromolecular solutions, J. Polym. Sci., Polym. Phys. Ed., 19 (1981) 479.
22 A.G. Ogston and E.F. Woods, The sedimentation of some fractions of degraded Dextran, Trans. Faraday Soc., 50 (1954) 635.
23 F.R. Senti, N.N. Hellman, N.H. Ludwig, G.E. Babcock, R. Tobin, C.A. Glass and B.L. Lamberts, Viscosity, sedimentation and light-scattering properties of fractions of an acid-hydrolyzed Dextran, J. Polym. Sci., 17 (1955) 527.
24 J.W. Williams and W.M. Saunders, Size distribution analysis in plasma extender systems. II. Dextran, J. Phys. Chem., 58 (1954) 854.